Eur. Phys. J. D **17**, 153–165 (2001)

THE EUROPEAN PHYSICAL JOURNAL D

EDP Sciences

Electromagnetically induced transparency and evolution of a two-level system under chaotic field of arbitrary intensity

A.G. Kofman[a]

Chemical Physics Department, Weizmann Institute of Science, Rehovot 76100, Israel

Received 31 December 2000 and Received in final form 14 May 2001

Abstract. The electromagnetically induced transparency (EIT) with a (near-)resonant chaotic (amplitude-phase fluctuating, Gaussian-Markovian) coupling field is studied theoretically. The Fourier transform of the steady-state EIT spectrum, which determines a nonstationary probe absorption, is also considered. This quantity equals the average diagonal element of the (reduced) evolution operator of the coupled transition (the evolution function). The exact solution in the form of a continued fraction is obtained and used to perform numerical calculations. Moreover, a number of approximate analytical results are obtained, which, together with the results of previous publications, describe the EIT and the evolution function in all possible regimes. In particular, in the constructive-interference case the EIT *increases* with the coupling-field bandwidth ν at sufficiently small ν. For a strong field, the maximum of the transparency as a function of ν is less than that for a monochromatic field of the same average intensity. In contrast, for a weak field, there is a range of ν values, where the field fluctuations *do not affect* the EIT. The latter result is shown to hold for a broad class of stochastic fields.

PACS. 42.50.Gy Effects of atomic coherence on propagation, absorption, and amplification of light – 42.50.Md Optical transient phenomena: quantum beats, photon echo, free-induction decay, dephasings and revivals, optical nutation, and self-induced transparency – 42.60.Mi Dynamical laser instabilities; noisy laser behavior

1 Introduction

The electromagnetically induced transparency (EIT) is a nonlinear optical phenomenon, involving quantum interference [1], which is of significant interest for both the fundamental science and the applied research [2]. Generally, the stronger the field producing the EIT the better the transparency. Since powerful lasers are often noisy, studies of effects of random fluctuations on the EIT are warranted. In comparison to Markovian phase fluctuations, which are well studied [3,4], the effects of amplitude-phase fluctuations on the EIT are less understood, though they are generally more significant and diverse [3,5–10].

Two related quantities are studied here. The first quantity is the steady-state EIT with an amplitude-phase fluctuating coupling field. The field is assumed to be chaotic, *i.e.*, its amplitude is a complex Gaussian-Markovian process. The second quantity is the Fourier transform of the EIT spectrum (the evolution function). This function determines the absorption of a time-dependent probe field and, moreover, has the meaning of the average diagonal element of the (reduced) evolution operator of of a two-level system driven by a chaotic field [10] (the average nondiagonal elements of the evolution operator will be shown to vanish).

[a] e-mail: abraham.kofman@weizmann.ac.il

The present problem involves five parameters: the coupling-field rms Rabi frequency, bandwidth, and detuning, and two relaxation constants. Four of the above parameters are independent (the fifth one defines the time and frequency scales). Correspondingly, many qualitatively different regimes are possible. Though some of the present results hold for an arbitrary coupling-field detuning, here the attention is focused on the (near-)resonance case, where the detuning vanishes or is relatively small. This reduces the number of independent parameters to three, the problem still remaining complicated.

Recently we studied the EIT in different regimes: the destructive-interference [8], constructive-interference [9], and relaxationless [10] cases. However, the previous studies were not complete. In particular, reference [9] is a preliminary report, which omits a number of interesting cases and necessary derivations, whereas the evolution function was not discussed in references [8,9]. Moreover, in reference [10] the validity conditions of the results were not obtained.

The purpose of the present study is twofold. First, the exact solution in the form of a continued fraction will be derived. Second, we shall obtain approximate analytical solutions for all unsolved cases and thus provide the comprehensive picture for the behaviour of the EIT and the evolution function in the (near-)resonance case. In

particular, we shall find the necessary and sufficient conditions for all regimes. Numerical calculations, using the above continued fraction, will be performed to corroborate the analytical results and to obtain the crossover between different regimes.

The constructive-interference case is given here a special consideration. In this case, a strong coupling field is known to induce a relatively narrow spectral peak between the components of the Autler-Towns doublet[1] [9]. Moreover, the following remarkable features are revealed below. (a) The *EIT increases with the bandwidth* for sufficiently narrowband coupling fields. (b) For a weak coupling field there is a range of the values of the bandwidth, where *the field fluctuations do not affect the EIT spectrum and the evolution function*, *i.e.*, the random field behaves as a monochromatic one.

The emphasis below is made on the new results, the previous results being mentioned briefly where it is necessary. The paper is organized as follows. In Section 2 the general formalism is presented. Section 3 provides the derivation of the continued-fraction solution. In Section 4 we present analytical results for the limiting cases of narrow- and broadband fields and show the applicability of these results to stochastic models more general than the chaotic field. An analytical solution for the constructive interference case is obtained in Section 5. In Section 6 we discuss analytical and numerical results for the EIT and the evolution function in various regimes. Section 7 provides the concluding remarks. Two appendices describe details of calculations.

2 Formulation of the problem

Consider a three-level atom with the ground state $|g\rangle$ and the excited states $|a\rangle$ and $|b\rangle$. The electromagnetically induced transparency (EIT) is observed in the absorption spectrum of a weak probe field near-resonant to the dipole-allowed transition $|g\rangle - |a\rangle$, whereas $|a\rangle$ and $|b\rangle$ are coupled by a strong laser field $E_{\rm c}(t)\mathrm{e}^{-\mathrm{i}\omega_{\rm c}t} + \text{c.c.}$ with the frequency $\omega_{\rm c}$ and the amplitude $E_{\rm c}(t)$. The excited levels $|a\rangle$ and $|b\rangle$ are assumed to be empty in the absence of the probe field.

The probe field with the frequency ω and the amplitude $E_{\rm p}(t)$ induces the polarization (the dipole moment per unit volume) $P(t)\mathrm{e}^{-\mathrm{i}\omega t} + P^*(t)\mathrm{e}^{\mathrm{i}\omega t}$. As shown in [8], the average polarization amplitude is

$$\bar{P}(t) = \frac{\mathrm{i}N|d_{ag}|^2}{\hbar}\int_0^t \mathrm{d}t'\mathrm{e}^{\mathrm{i}\Delta(t-t')}\bar{U}_{aa}(t-t')E_{\rm p}(t'), \quad (2.1)$$

which implies that the steady-state absorption spectrum for a cw probe field [$E_{\rm p}(t) = \text{const.}$] is given by

$$\bar{A}(\Delta) = \mathrm{Re}\int_0^\infty \mathrm{d}t\,\bar{U}_{aa}(t)\mathrm{e}^{\mathrm{i}\Delta t}. \quad (2.2)$$

[1] Similar three-peak lineshapes were found for double optical resonance with an intensity fluctuating field [11] and for normal-mode line shapes of high-Q cavities, wherein the source of fluctuations is the intracavity atomic number [12].

Here $\Delta = \omega - \omega_{ag}$ is the probe field detuning, the overbar denotes averaging over random fluctuations of the coupling field, N is the number of the atoms under consideration per unit volume, d_{ij} is the dipole matrix element for transition $|i\rangle - |j\rangle$, and $\bar{A}(\Delta) = \bar{\alpha}(\omega)/K$ is the scaled average absorption coefficient, where $\omega_{ij} = \omega_i - \omega_j$, $\hbar\omega_i$ is the energy of level $|i\rangle$, $\bar{\alpha}(\omega)$ is the average absorption coefficient, and $K = 4\pi N\omega|d_{ag}|^2/(\hbar c)$ with c being the vacuum speed of light. Equation (2.2) holds if $\bar{\alpha}(\omega)L \ll 1$, where L is the sample thickness along the propagation direction of the probe field [8]. For definiteness, below we consider the ladder scheme ($\omega_b > \omega_a$). The results for the Λ-scheme ($\omega_b < \omega_a$) follow from those for the ladder scheme with the help of the substitutions (2.14) in [8].

The quantity $\bar{U}_{aa}(t)$ is the averaged solution of the Schrödinger equation [3,8]

$$\mathrm{i}\dot{U} = \begin{pmatrix} -\mathrm{i}\Gamma & V_{\rm c}^*(t) \\ V_{\rm c}(t) & -\Delta_{\rm c} - \mathrm{i}\Gamma' \end{pmatrix} U \quad (2.3)$$

for the operator $U_{ij}(t)$ with the initial condition $U_{ij}(0) = \delta_{ij}$, where $i, j = a, b$ and δ_{ij} is the Kronecker symbol. In equation (2.3) $V_{\rm c}(t) = -d_{ba}E_{\rm c}(t)/\hbar$ and $\Delta_{\rm c} = \omega_{\rm c} - \omega_{ba}$ is the coupling-field detuning, whereas Γ and Γ' are the homogeneous HWHM widths of the transitions $|g\rangle - |a\rangle$ and $|g\rangle - |b\rangle$, respectively.

Note that equation (2.3) results from the equations for the density matrix elements ρ_{ag} and ρ_{bg} [8]. Since in the present weak-probe approximation the amplitude of $|g\rangle$ is close to one, ρ_{ag} and ρ_{bg} behave as the amplitudes of $|a\rangle$ and $|b\rangle$. This explains why equation (2.3) has the form of the Schrödinger equation.

As discussed in [10], $U(t)$ is generally the operator of the reduced evolution of the TLS $\{|a\rangle, |b\rangle\}$ (*i.e.*, the evolution of the subensemble with no spontaneous transitions between $|a\rangle$ and $|b\rangle$ [13]) averaged over collision-induced random phase shifts. In those cases, when the rates of the above spontaneous transitions and the dephasing collisions are negligible small, $U(t)$ is just the evolution operator of the above TLS.

Thus, equation (2.2) establishes the relation between the EIT spectrum and the evolution of TLS $\{|a\rangle, |b\rangle\}$. Conversely, the evolution function $\bar{U}_{aa}(t)$ can be expressed through the EIT spectrum [10],

$$\bar{U}_{aa}(t) = \frac{1}{\pi}\int_{-\infty}^{\infty} \bar{A}(\Delta)\mathrm{e}^{-\mathrm{i}\Delta t}\mathrm{d}\Delta. \quad (2.4)$$

Relations (2.2) and (2.4) allow us to study the EIT and the average evolution of the TLS simultaneously below.

Note that $\bar{U}_{aa}(t)$ is of interest both in its own right and because it directly defines the absorption rate of the probe field when $E_{\rm p}(t)$ depends on time. The latter follows from equation (2.1) and the fact that the average absorption rate is proportional to $\mathrm{Im}E_{\rm p}^*(t)\bar{P}(t)$ [14].

Henceforth we consider a chaotic coupling field, *i.e.*, a complex Gaussian-Markovian random process $E_{\rm c}(t)$ or $V_{\rm c}(t)$. Chaotic field has the vanishing average and an exponential correlation function, $k(t) \equiv \overline{V_{\rm c}^*(t+\tau)V_{\rm c}(\tau)} = V_0^2\mathrm{e}^{-\nu|t|}$, where V_0 is the rms Rabi frequency, $V_0^2 = \overline{|V_{\rm c}|^2}$,

and ν^{-1} is the correlation time of the coupling field. Correspondingly, the coupling-field bandshape is Lorentzian with the HWHM width ν. The complex coupling amplitude $V_c = u + iv$ of the chaotic field has a Gaussian distribution $dW(\mathbf{V}) = f(V)d\mathbf{V}$. Here $\mathbf{V} = (u, v)$, $d\mathbf{V} = dudv$, $V = |V_c|$ is the Rabi frequency of the chaotic field, and

$$f(V) = \exp(-V^2/V_0^2)/\pi V_0^2. \tag{2.5}$$

Consider the partially averaged evolution operator $U(\mathbf{V}, t)$ [8]. The Laplace transforms $\Psi_i(\mathbf{V}) = \int_0^\infty U_{ia}(\mathbf{V}, t)e^{i\Delta t}dt$ $(i = a, b)$ satisfy the following equations [8],

$$-\tilde{\Gamma}\Psi_a - iV_c^*\Psi_b + L\Psi_a = -f(V), \tag{2.6a}$$
$$-\tilde{\Gamma}'\Psi_b - iV_c\Psi_a + L\Psi_b = 0, \tag{2.6b}$$

Here $\tilde{\Gamma} = \Gamma - i\Delta$, $\tilde{\Gamma}' = \Gamma' - i\Delta'$, where $\Delta' = \Delta + \Delta_c$, and the stochastic operator $L = L_u + L_v$ takes into account temporal fluctuations of the coupling field, where L_u and L_v are defined by

$$L_u = \nu\left(1 + u\frac{\partial}{\partial u} + \frac{V_0^2}{2}\frac{\partial^2}{\partial u^2}\right). \tag{2.7}$$

The fully averaged quantity

$$\bar{\Psi}_i = \int \Psi_i(\mathbf{V})d\mathbf{V} = \int_0^\infty \bar{U}_{ia}(t)e^{i\Delta t}dt. \tag{2.8}$$

The probe absorption spectrum can be written now as

$$\bar{A}(\Delta) = \mathrm{Re}\bar{\Psi}_a. \tag{2.9}$$

3 Continued-fraction solution

The average solution of equation (2.3) can be obtained with the help of the generalized cumulant expansion [15–17]. As a result, one obtains for a chaotic $V_c(t)$ that

$$\bar{U}_{ba}(t) = \bar{U}_{ab}(t) = 0, \tag{3.1}$$

whereas the Laplace transform

$$\hat{\bar{U}}_{aa}(s) = \int_0^\infty dt\, e^{-st}\bar{U}_{aa}(t) \tag{3.2}$$

of $\bar{U}_{aa}(t)$ is given by

$$\hat{\bar{U}}_{aa}(s) = \left[s + \Gamma + \sum_{k=1}^{\infty}(-1)^{k+1}Q_k(s)\right]^{-1}. \tag{3.3a}$$

Here

$$Q_k(s) = \int_0^\infty d\tau_1 ... \int_0^\infty d\tau_{2k-1} \exp\left[-\sum_{i=1}^{2k-1}(s + p_i)\tau_i\right] \times d_k(\tau_1 + ... + \tau_{2k-1}, ..., \tau_1, 0), \tag{3.3b}$$

where $p_{2j} = \Gamma$, $p_{2j-1} = \Gamma' - i\Delta_c \equiv \Gamma_c$ $(j = 1, 2, ...)$, and $d_k(t_1, ..., t_{2k}) = PV_1^*V_2QV_3^*V_4...QV_{2k-1}^*V_{2k}$. Here P is the averaging operator, $Q = 1 - P$, and $V_j = V(t_j)$.

In particular, for the chaotic field $d_1 = V_0^2\kappa_{11}$, $d_2 = V_0^4\kappa_{11}\kappa_{22}\kappa_{13}$, $d_3 = V_0^6\kappa_{11}\kappa_{22}(\kappa_{13} + 2\kappa_{33})\kappa_{24}\kappa_{15}$, $d_4 = V_0^8\kappa_{11}\kappa_{22}(\kappa_{13}\kappa_{24}\kappa_{15} + 2\kappa_{33}\kappa_{24}\kappa_{15} + 2\kappa_{13}\kappa_{24}\kappa_{35} + 4\kappa_{33}\kappa_{24}\kappa_{35} + 4\kappa_{33}\kappa_{44}\kappa_{35})\kappa_{26}\kappa_{17}$, where $\kappa_{jk} = e^{-j\nu\tau_k}$ and $\tau_k = t_k - t_{k+1}$. Hence

$$Q_1(s) = V_0^2 b_1, \quad Q_2(s) = V_0^4 b_1 a_2,$$
$$Q_3(s) = V_0^6 b_1^2 a_2^2(b_1 + 2b_3),$$
$$Q_4(s) = V_0^8 b_1^2 a_2^2(b_1^2 a_2 + 4b_1 a_2 b_3 + 4b_3^2 a_2 + 4b_3^2 a_4), \tag{3.4}$$

where $a_n = (s + \Gamma + n\nu)^{-1}$ and $b_n = (s + \Gamma_c + n\nu)^{-1}$.

To recast the expansion (3.3a) as a continued fraction, we note that in the case

$$\Gamma = \Gamma' = \Delta_c = 0 \tag{3.5}$$

the relaxation function $\bar{U}_{aa}(t)$ can be shown to coincide, up to a renormalization of V_0, with the average population difference $\bar{n}(t)$ of a TLS driven by a chaotic field [18]. Correspondingly, the cumulant expansions for the Laplace transforms of $\bar{U}_{aa}(t)$ (Eqs. (3.3a) and (3.4)) and $\bar{n}(t)$ [19] are similar. In the general case, the above two quantities behave quite differently: $\bar{n}(t)$ is always real, whereas $\bar{U}_{aa}(t)$ can be complex. However, the form of the two expansions is preserved, by continuity, also for the general case. Indeed, expansion (3.3a) and (3.4) and that in reference [19] can be formally identified if the parameters $\hat{c}_n$ and $\hat{u}_n$ introduced in [19] are redefined by $\hat{c}_n = ib_n$ and $\hat{u}_n = ia_n$. This allows us to use the continued fraction given by equations (4.5–4.8) in [19] for the summation of expansion (3.3a) and (3.4). As a result, $\bar{\Psi}_a = \hat{\bar{U}}_{aa}(-i\Delta)$ (see Eq. (2.8)) is given by

$$\bar{\Psi}_a = (\tilde{\Gamma} + D_1)^{-1}, \tag{3.6a}$$

where $(n = 1, 2, ...)$

$$D_n = \frac{V_0^2}{\tilde{\Gamma}' + (2n-1)\nu + V_0^2/(\tilde{\Gamma} + 2n\nu + D_{n+1})}. \tag{3.6b}$$

In view of equations (2.9, 2.4), the continued fraction (3.6) allows one to compute the EIT spectrum and the evolution function $\bar{U}_{aa}(t)$ *for all possible values of the parameters.*

Below we focus on the case of a moderate detuning,

$$|\Delta_c| \lesssim \Gamma + \Gamma'. \tag{3.7}$$

We shall assume also that

$$V_0^2 \gtrsim \Gamma\Gamma', \tag{3.8}$$

which is a necessary condition for the probe absorption to be significantly modified by the coupling field [8].

4 Limiting cases

In the limiting cases of very narrow- and broadband fields one can obtain analytical results, whose applicability is much broader than the chaotic field model, as noted below.

4.1 Static limit

4.1.1 EIT

For a very narrowband field, $\nu \to 0$, one can neglect $L\Psi_a$ in equations (2.6) and solve the resulting algebraic equations to obtain [8]

$$\bar{A}(\Delta) = V_0^{-2}\mathrm{Re}\tilde{\Gamma}'\mathrm{e}^{\tilde{\Gamma}\tilde{\Gamma}'/V_0^2}E_1(\tilde{\Gamma}\tilde{\Gamma}'/V_0^2), \tag{4.1}$$

where $E_1()$ is the integral exponential function [20]. In the case (3.5) the spectrum (4.1) is the broadened Autler-Towns doublet [3,5,10],

$$\bar{A}(\Delta) = \pi V_0^{-2}|\Delta|\exp(-\Delta^2/V_0^2). \tag{4.2}$$

4.1.2 TLS evolution

For a coherent coupling field, $V_\mathrm{c}(t) = \mathrm{const.}$, a solution of equation (2.3) yields,

$$U_{aa}(t) = \exp\left(-\frac{\Gamma+\Gamma_\mathrm{c}}{2}t\right)\left(\cos\Omega t + \frac{\Gamma_\mathrm{d}}{2\Omega}\sin\Omega t\right), \tag{4.3}$$

where $\Gamma_\mathrm{d} = \Gamma_\mathrm{c} - \Gamma$ and $\Omega = \sqrt{V^2 - \Gamma_\mathrm{d}^2/4}$. In the static limit, $\bar{U}_{aa}^{\mathrm{st}}(t) = \int U_{aa}(t)f(\mathbf{V})\mathrm{d}\mathbf{V}$. Inserting equation (4.3) here and performing the integration yields, after some algebra,

$$\begin{aligned}\bar{U}_{aa}^{\mathrm{st}}(t) = {} & \tfrac{\mathrm{e}^{-\Gamma t}+\mathrm{e}^{-\Gamma_\mathrm{c}t}}{2} - \left(\tfrac{V_0 t}{2} - \tfrac{\Gamma_\mathrm{d}}{2V_0}\right) \\ & \times\left[\mathrm{e}^{-\Gamma t}F\left(\tfrac{V_0 t}{2} + \tfrac{\Gamma_\mathrm{d}}{2V_0}\right)\right. \\ & \left.+\mathrm{e}^{-\Gamma_\mathrm{c}t}F\left(\tfrac{V_0 t}{2} - \tfrac{\Gamma_\mathrm{d}}{2V_0}\right)\right],\end{aligned} \tag{4.4}$$

where [20] $F(z) = \mathrm{e}^{-z^2}\int_0^z \mathrm{d}y\,\mathrm{e}^{y^2}$.

For the case (3.5) equation (4.4) becomes [5]

$$\bar{U}_{aa}^{\mathrm{st}}(t) = 1 - V_0 t F(V_0 t/2). \tag{4.5}$$

This function has the following limits [10]: $\bar{U}_{aa}^{\mathrm{st}}(t) \approx 1 - V_0^2 t^2/2$ ($t \ll V_0^{-1}$) and $\bar{U}_{aa}^{\mathrm{st}}(t) \approx -2/V_0^2 t^2$ ($t \gg V_0^{-1}$).

Note that the results of the static limit hold in the limit $\nu \to 0$ for any intensity-fluctuating field with the distribution (2.5).

4.2 Broadband limit

In this subsection we consider a rather general class of phase, amplitude, and amplitude-phase fluctuating fields, as specified below.

We start by noting that equation (3.3) holds for any stochastic field with vanishing odd moments. As follows from the above definition of the cumulant $d_k(\tau_1 + ... + \tau_{2k-1}, ..., \tau_1, 0)$, it tends to zero for each τ_i tending to infinity. Assuming that this decay occurs exponentially or faster with the rate of the order of the field bandwidth ν, as is the case for a chaotic field (*cf.* Sect. 3), one can estimate that

$$|Q_k(s)| \sim V_0^{2k}/|(s+\Gamma+\nu)^{k-1}(s+\Gamma_\mathrm{c}+\nu)^k|. \tag{4.6}$$

The series in equation (3.3a) converges fast when $|Q_{k+1}(s)|/|Q_k(s)| \sim V_0^2/|(s+\Gamma+\nu)(s+\Gamma_\mathrm{c}+\nu)| \ll 1$. We are interested in the case of an imaginary $s = -\mathrm{i}\Delta$, when the spectrum $\bar{A}(\Delta) = \mathrm{Re}\hat{\bar{U}}_{aa}(-\mathrm{i}\Delta)$ is obtained. In the region (3.7), the above ratio is maximal when $\Delta = 0$, yielding the condition $V_0^2 \ll (\Gamma+\nu)(\Gamma'+\nu)$. Restricting our attention to the case (3.8), the latter condition can be recast as

$$V_0^2 \ll \nu(\Gamma+\Gamma'+\nu). \tag{4.7}$$

Under condition (4.7), one can approximate the sum in equation (3.3a) by its first term, yielding in the first approximation

$$\bar{A}(\Delta) = \mathrm{Re}[\tilde{\Gamma} + \hat{k}(\tilde{\Gamma}')]^{-1}, \tag{4.8}$$

where $\hat{k}(s)$ is the Laplace transform of the correlation function $k(t) = \overline{V_\mathrm{c}^*(t)V_\mathrm{c}(0)}$. Inequality (4.7) implies that the main part of the EIT spectrum (4.8), except for far wings, is Lorentzian,

$$\bar{A}(\Delta) = \frac{\Gamma+w}{(\Gamma+w)^2+(\Delta-\delta)^2} \qquad (|\Delta| \ll \nu+\Gamma'), \tag{4.9}$$

where $w = \mathrm{Re}\hat{k}(\Gamma_\mathrm{c})$ and $\delta = \mathrm{Im}\hat{k}(\Gamma_\mathrm{c})$ are the field-induced spectral width and shift.

The spectrum simplifies in two cases. For $\nu \gg \Gamma'$, one can set in equation (4.8) $\hat{k}(\tilde{\Gamma}') \approx \hat{k}(-\mathrm{i}\Delta)$. As regards equation (4.9), one obtains $w \approx \hat{k}(0) \equiv V_0^2/\nu$ (the latter equality defining ν for the general case), whereas $|\delta| \sim V_0^2|\Delta_\mathrm{c}|/\nu^2 \ll w$, yielding

$$\bar{A}(\Delta) = \frac{\Gamma + V_0^2/\nu}{(\Gamma + V_0^2/\nu)^2 + \Delta^2} \qquad (|\Delta| \ll \nu). \tag{4.10}$$

For $\nu \ll \Gamma'$ one obtains $\hat{k}(\tilde{\Gamma}') \approx V_0^2/\tilde{\Gamma}'$ and equation (4.8) becomes

$$\bar{A}(\Delta) = \mathrm{Re}[\Gamma - \mathrm{i}\Delta + V_0^2/(\Gamma' - \mathrm{i}\Delta')]^{-1}. \tag{4.11}$$

The main part ($|\Delta| \ll \Gamma'$) of the spectrum (4.11) is Lorentzian, equation (4.9), with $w = V_0^2\Gamma'/(\Gamma'^2 + \Delta_\mathrm{c}^2)$ and $\delta = V_0^2\Delta_\mathrm{c}/(\Gamma'^2 + \Delta_\mathrm{c}^2)$. In this case, a stochastic coupling field affects the spectrum in the same manner as a *monochromatic* field with the same average intensity. As follows from equations (3.8) and (4.7), the above regime holds for $\Gamma \ll \Gamma'$ and $V_0^2 \ll \nu\Gamma'$.

For a field with a Lorentzian bandshape, as, *e.g.*, a chaotic field, the spectrum (4.8) acquires the form

$$\bar{A}(\Delta) = \mathrm{Re}[\Gamma - \mathrm{i}\Delta + V_0^2/(\Gamma' + \nu - \mathrm{i}\Delta')]^{-1}. \tag{4.12}$$

This spectrum is the same as for a field with Markovian phase fluctuations [3,4,8]. The main part of the spectrum has the form (4.9) with

$$w = \frac{V_0^2(\nu+\Gamma')}{(\nu+\Gamma')^2+\Delta_\mathrm{c}^2}, \quad \delta = \frac{V_0^2\Delta_\mathrm{c}}{(\nu+\Gamma')^2+\Delta_\mathrm{c}^2}\cdot \tag{4.13}$$

The expansion (3.3) can be used also to obtain far wings of the spectrum for the general case, irrespective of condition (4.7). In particular, for the chaotic-field case, on truncating the sum in (3.3) after the second term, one can obtain the exact expansion of the spectrum for large $|\Delta|$ up to Δ^{-6}. Neglecting small terms in this expansion yields in the first approximation

$$\bar{A}(\Delta) \approx \frac{\Gamma}{\Delta^2} + \frac{V_0^2(\nu+\Gamma')}{\Delta^4} \quad (|\Delta| \gg V_0, \nu, \Gamma, \Gamma'). \quad (4.14)$$

The very far wings of the spectrum are the same as in the absence of the coupling field (see the first term in Eq. (4.14)). However for moderately large $|\Delta|$ the second term in (4.14) may dominate.

The inverse transform (2.4) of equation (4.9) yields an exponential evolution, except for very short times,

$$\bar{U}_{aa}(t) = \mathrm{e}^{-[\Gamma+\hat{k}(\Gamma_\mathrm{c})]t} \qquad \left(t \gg (\nu+\Gamma')^{-1}\right). \quad (4.15)$$

In particular, for a field with a Lorentzian bandshape, equation (4.15) implies

$$\bar{U}_{aa}(t) = \mathrm{e}^{-[\Gamma+V_0^2/(\Gamma_\mathrm{c}+\nu)]t} \qquad \left(t \gg (\nu+\Gamma')^{-1}\right). \quad (4.16)$$

5 Analytical solution

The set of second-order differential equations (2.6) cannot be solved in a closed form for the most general case. However equations (2.6) can be solved analytically, on omitting either $L\Psi_a$ or $L\Psi_b$. Whereas the former case was considered in detail in [8], the latter case can be treated as follows.

When Γ' or $|\Delta'|$ is sufficiently large, one can neglect the term $L\Psi_b$ in equations (2.6b). Then one obtains

$$\Psi_b(\mathbf{V}) = -\mathrm{i}V_\mathrm{c}\Psi_a/(\Gamma' - \mathrm{i}\Delta'). \quad (5.1)$$

Inserting equation (5.1) into (2.6a) yields the equation for Ψ_a

$$(\mathrm{i}\Delta - \Gamma)\Psi_a - \frac{V^2}{\Gamma' - \mathrm{i}\Delta'}\Psi_a + L\Psi_a = -f(V). \quad (5.2)$$

The solution of equation (5.2) is

$$\Psi_a(\mathbf{V}) = \int_0^\infty g(\mathbf{V},t)\mathrm{e}^{-(\Gamma-\mathrm{i}\Delta)t}\mathrm{d}t, \quad (5.3)$$

where $g(\mathbf{V},t)$ obeys the equation

$$\dot{g} = -[V^2/(\Gamma' - \mathrm{i}\Delta')]g + Lg \quad (5.4)$$

with the initial condition $g(\mathbf{V},0) = f(V)$. Correspondingly,

$$\bar{\Psi}_a = \int_0^\infty \bar{g}(t)\mathrm{e}^{-(\Gamma-\mathrm{i}\Delta)t}\mathrm{d}t, \quad (5.5)$$

where $\bar{g}(t) = \int g(\mathbf{V},t)\,\mathrm{d}\mathbf{V}$.

The solution of an equation of the form (5.4) was obtained repeatedly [21,22], being

$$g(\mathbf{V},t) = \frac{\beta_0}{\pi V_0^2 R_0(t)} \exp\left[\nu t - \frac{S(\beta_0,t)V^2}{2V_0^2 R_0(t)}\right], \quad (5.6)$$

where $\beta_0 = [1 + 2V_0^2/\nu(\Gamma' - \mathrm{i}\Delta')]^{1/2}$, $R_0(t) = \beta_0\cosh\beta_0\nu t + \sinh\beta_0\nu t$, and $S(\beta_0,t) = 2\beta_0\cosh\beta_0\nu t + (1+\beta_0^2)\sinh\beta_0\nu t$. Hence $\bar{g}(t) = 2\beta_0\mathrm{e}^{\nu t}/S(\beta_0,t)$. Inserting the latter result into (5.5) and performing the integration yields finally that the spectrum (2.9) is

$$\bar{A}(\Delta) = \mathrm{Re}\frac{F(1,1;1+d_0;-z_0)}{\Gamma - \mathrm{i}\Delta + (\beta_0-1)\nu}, \quad (5.7)$$

where $F()$ is the hypergeometric function [20], $d_0 = [\tilde{\Gamma} + (\beta_0-1)\nu]/2\beta_0\nu$, and $z_0 = (\beta_0-1)^2/4\beta_0$. The validity conditions of equation (5.7) are shown in Appendix A to be

$$\sqrt{V_0^2\nu} \ll (\Gamma' + |\Delta'|)\left(\sqrt{\Gamma+|\Delta|} + \sqrt{\Gamma'+|\Delta'|}\right), \quad (5.8a)$$

$$\nu \ll \Gamma' + |\Delta'|. \quad (5.8b)$$

Equation (5.7) can be simplified in two cases. Using the hypergeometric-function expansion (15.3.13) in [20] yields [9]

$$\bar{A}(\Delta) = \mathrm{Re}\frac{\tilde{\Gamma}'}{V_0^2}\left[\frac{1}{2}\ln\frac{C_1^2V_0^2}{8\nu\tilde{\Gamma}'} - \psi\left(a_0+\frac{1}{2}\right)\right]. \quad (5.9)$$

Here $\psi()$ is the logarithmic derivative of the Γ-function[20], $a_0 = \tilde{\Gamma}[\tilde{\Gamma}'/(8V_0^2\nu)]^{1/2}$, and $C_1 = \mathrm{e}^{-\gamma} \approx 0.56$, where γ is the Euler constant [20]. The smallness parameter of the above expansion is $(1+|d_0|)/|z_0|$. This implies the validity conditions of equation (5.9) to be

$$V_0^2 \gg (\Gamma+|\Delta|)(\Gamma'+|\Delta'|), \quad (5.10a)$$

$$V_0 \gg \sqrt{\nu(\Gamma'+|\Delta'|)}. \quad (5.10b)$$

When $|z_0| \ll 1 + |d_0|$, which implies, in the frame of the validity conditions (5.8), the inequality

$$V_0^2 \ll \nu(\Gamma'+|\Delta'|), \quad (5.11)$$

one obtains that $F(1,1;1+d_0;-z_0) \approx 1$ and $\beta_0 \approx 1 + V_0^2/\nu\tilde{\Gamma}'$, equation (5.7) becoming (4.11).

The above results in this section hold for an arbitrary Δ_c. For the near-resonant case, $|\Delta_\mathrm{c}| \lesssim \Gamma'$, the validity conditions (5.8) of equation (5.7) hold for all $|\Delta|$ if

$$(a)\ \sqrt{V_0^2\nu} \ll \Gamma'^{3/2}, \quad (b)\ \nu \ll \Gamma'. \quad (5.12)$$

The solution (5.7) and condition (5.12a) were presented without derivation in [9].

6 Results and discussion

In this section we study different regimes for the EIT and the evolution function in the near-resonant case (3.7).

We shall show that the formulas obtained here and in references [8–10] describe analytically all possible situations. We begin with defining the boundaries of different regimes.

Note first that the necessary and sufficient conditions for the probe absorption to be significantly modified by the coupling field are equation (3.8) and the relation

$$V_0^2 \gtrsim \Gamma\nu, \tag{6.1}$$

which is implied by equation (4.10).

The static limit (Sect. 4.1) holds for [8,9]

$$V_0^2\nu \ll \Gamma_+\Gamma_-^2, \tag{6.2}$$

where $\Gamma_+ = \max\{\Gamma, \Gamma'\}$ and $\Gamma_- = \min\{\Gamma, \Gamma'\}$. The results of references [8,9] are valid for (*cf.* Eq. (5.12))

$$\text{(a)}\ \sqrt{V_0^2\nu} \ll \Gamma_+^{3/2}, \qquad \text{(b)}\ \nu \ll \Gamma_+. \tag{6.3}$$

The limits of all the possible regimes are shown in Figure 1. In regions IV and V the broadband-limit results hold, since boundaries 4 and 5 correspond to condition (4.7).

Below the new results are discussed in detail, whereas the previous results are mentioned, for completeness, only briefly. The numerical results, for simplicity, will be shown for the case of exactly resonant coupling field, $\Delta_c = 0$. In this case, as follows from equation (3.6), the EIT spectrum (2.9) is symmetric with respect to the inversion of the sign of Δ, which allows one to recast equation (2.4) in the form

$$\bar{U}_{aa}(t) = \frac{2}{\pi}\mathrm{Re}\int_0^\infty \bar{A}(\Delta)\mathrm{e}^{-\mathrm{i}\Delta t}\mathrm{d}\Delta. \tag{6.4}$$

6.1 Relaxationless case

The case when the relaxation constants and detuning can be neglected, equation (3.5), was studied thoroughly in [10]. This case is shown below to be realized in regions III and IV (except for far wings, (4.14), which we shall ignore below). In particular, in region III the spectrum has the form (4.2), except for the central part, which is smoothed, so that the minimum absorption $\bar{A}(0) = 1.728\nu^{1/3}V_0^{-4/3}$. The evolution function in region III is described by equation (4.5) for sufficiently short times, until the exponential cutoff at $t \sim (V_0^2\nu)^{-1/3}$, which is the characteristic time of the irreversible relaxation [10]. In region IV, the spectrum is a Lorentzian peak, whereas the evolution function decays exponentially. They are described by equations (4.10) and (4.16), where the relaxation constants can be neglected (see Ref. [10], Eqs. (4.11, 4.13)). With approaching and traversing boundary 6, $\nu \gtrsim V_0^2/\Gamma$, one should retain Γ in equations (4.10) and (4.16), which allows one to describe the transition to the unperturbed results with an increase of ν (or a decrease of V_0).

Below we present analytical and numerical results for the EIT and the evolution function, the emphasis being on regions I, II, and V, where the behaviour significantly depends on the material relaxation. Analysis in

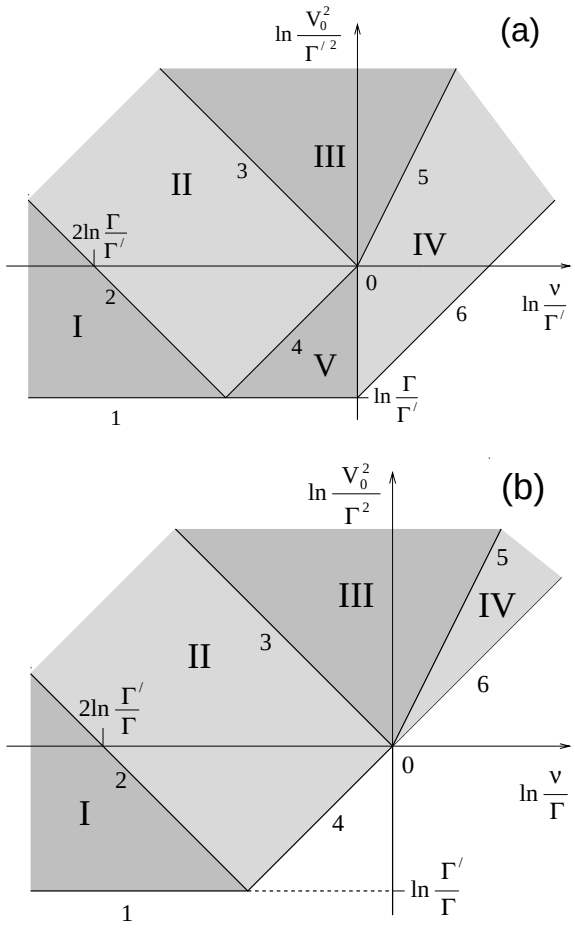

Fig. 1. The boundaries of different regimes in the parameter space for the near-resonance case $|\Delta_c| \lesssim \Gamma + \Gamma'$. (a) $\Gamma' \gg \Gamma$, (b) $\Gamma' \ll \Gamma$. Region I, the quasistatic regime; region II, the ν-dependent regime with strong interference; region III, relaxationless, narrowband regime; regions IV and V, the broadband limit. Boundaries 1–6 are defined by conditions (3.8, 6.2, 6.3a), $V_0^2 = \nu\Gamma_+$, $V_0^2 = \nu^2$, and (6.1), respectively.

references [8,9] showed that for $\Gamma \gg \Gamma'$ ($\Gamma \ll \Gamma'$) in the above regions the EIT is significantly affected by destructive (constructive) interference of the dressed states. Note that regions II and V exist only in the case of significantly nonequal relaxation constants [8,9]. In this case a significant EIT is possible for both strong and weak fields, $V_0^2 \gtrsim \Gamma + \Gamma'$ and $\Gamma\Gamma' \lesssim V_0^2 \ll (\Gamma + \Gamma')^2$, respectively.

6.2 Constructive interference ($\Gamma \ll \Gamma'$)

6.2.1 EIT spectrum

Consider first the static limit, $\nu \to 0$. The analysis of equation (4.1) [9] shows that the central part of the static spectrum is a peak with the shape given by a logarithm of a Lorentzian,

$$\bar{A}(\Delta) \approx \frac{\Gamma'}{2V_0^2}\ln\frac{C_1^2V_0^4}{\Gamma'^2(\Gamma^2 + \Delta^2)} \tag{6.5}$$

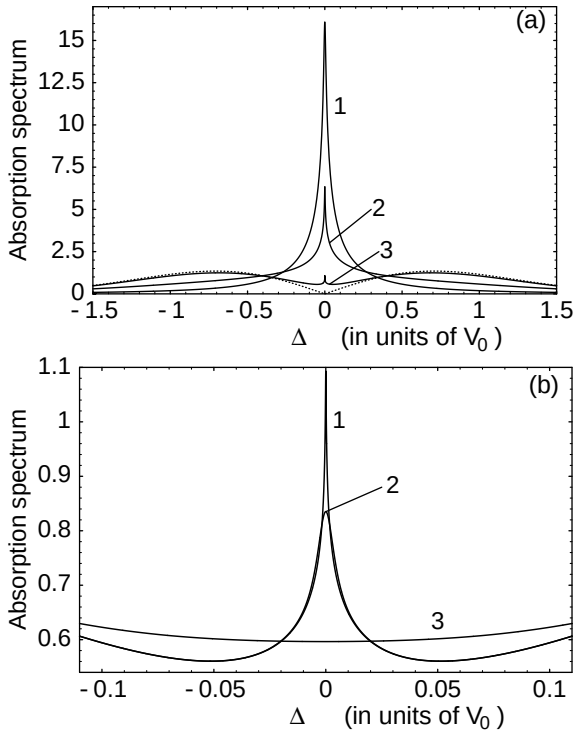

Fig. 2. The probe absorption spectrum $\bar{A}(\Delta)$ (in units of V_0^{-1}) for the constructive interference case, $\Gamma = 10^{-3}\Gamma'$, $\Delta_c = 0$. (a) The static-limit. Here $V_0/\Gamma' = 0.2$ (curve 1), 1 (curve 2), 10 (curve 3). Dotted line, $\Gamma = \Gamma' = \nu = 0$ (Eq. (4.2)). (b) ν dependence in the strong-field case. Here $V_0 = 10\Gamma'$ and $\nu/V_0 = 0$ (curve 1), 10^{-6} (curve 2), 1.5×10^{-3} (curve 3).

($|\Delta| \ll \min\{V_0, \Gamma'\}$). For weak ($V_0 \ll \Gamma'$) and intermediate ($V_0 \sim \Gamma'$) fields the spectrum has a single peak (6.5) (Fig. 2a, curves 1 and 2), whereas for strong fields ($V_0 \gg \Gamma'$) equation (6.5) describes a relatively narrow peak between the two broad Autler-Towns components (Fig. 2a, curve 3) [9]. The maximum of the peak (6.5) is at $\Delta = 0$, and the peak half width at half maximum (HWHM) equals $0.52\sqrt{\Gamma\Gamma'}$. Except for the central part, the strong-field spectrum is close to the relaxationless result (4.2) (*cf.* curve 3 and the dotted line in Fig. 2a).

The peak (6.5) has a narrower central part and slower decaying wings than the Lorentzian one. Note that the static spectrum (4.1) is obtained by averaging the EIT spectrum with a coherent coupling field, $A(\omega) = \mathrm{Re}(\tilde{\Gamma} + V^2/\tilde{\Gamma}')^{-1}$, over the distribution (2.5). The spectrum $A(\omega)$ can be shown to be the Autler-Towns doublet for $V \gg \Gamma'$ and a Lorentzian with the width $\Gamma + V^2\Gamma'/(\Gamma'^2 + \Delta_c^2)$ and shift $V^2\Delta_c/(\Gamma'^2 + \Delta_c^2)$ for $V \ll \Gamma'$. Since the distribution (2.5) is constant for $V \ll V_0$, the superposition of the above Lorentzians with $V \ll \min\{V_0, \Gamma'\}$ yields the peak (6.5).

Consider the transformation of the spectrum with the increase of ν. One can use now the above analytical solution (5.7). According to condition (5.12), the formula (5.7) holds in the regions I, II, and V in Figure 1a (note that Eq. (5.12a) defines boundary 3 in Fig. 1a). One can show with the help of equation (5.9) [9] that the static-limit results hold in region I, *i.e.*, for $V_0^2\nu \ll \Gamma^2\Gamma'$ (see Eq. (6.2) and boundary 2 in Fig. 1a).

In region II the peak height decreases with ν,

$$\bar{A}(\Delta) = \frac{\Gamma'}{2V_0^2} \ln \frac{2V_0^2}{\Gamma'\nu} \quad \left(|\Delta| \ll \sqrt{V_0^2\nu/\Gamma'}\right), \qquad (6.6)$$

whereas outside the vicinity of the maximum (for $\Delta^2 \gg V_0^2\nu/\Gamma'$) the spectral shape remains approximately quasistatic. Thus, in the present case *the transparency increases with the increase of the coupling-field bandwidth* [9]. Further transformation of the spectrum with ν occurs differently for the weak- and strong-field cases.

In the weak-field case, *i.e.*, below the horizontal axis in Figure 1a, the peak height diminishes with ν according to (6.6) in the interval $\Gamma^2\Gamma'/V_0^2 \ll \nu \ll V_0^2/\Gamma'$ (region II). When the latter inequality is inverted, the broadband limit occurs (*cf.* Eq. (4.7)) and the spectrum becomes Lorentzian, equations (4.9, 4.13). In the interval $V_0^2/\Gamma' \ll \nu \ll \Gamma'$ (region V in Fig. 1a) the spectrum practically does not depend on ν, being described by equation (4.11). The result (4.11) holds also for a monochromatic coupling field which has the same average intensity as the chaotic field. In other words, in the above region *the random fluctuations of the field do not affect the spectrum.* For $\nu \gg \Gamma'$ the spectrum is given by (4.10), as discussed above for region IV. The dependence of the peak hight on ν for a weak coupling field is shown in Figure 3a. The transformation of the spectrum with ν for the weak-field case was plotted in [7], Figure 6.

The present treatment has some overlap with reference [7], where the path-integral method was employed to study the constructive-interference, weak-field case. In particular, the result similar to equations (4.9, 4.13) was obtained ([7], Eqs. (39, 40)). Note, however, that many of the present results, including equations (4.9, 4.13), are shown in Section 4 to hold for a more general case than the chaotic-field model considered in reference [7].

The closed formulas (4.12) and (5.7) completely describe the EIT for a weak-field case, since their validity domains (4.7) and (5.12), respectively, overlap in region V ($V_0^2/\Gamma' \ll \nu \ll \Gamma'$), where the both results approximately reduce to equation (4.11). Alternatively, the above discussion implies that *in the weak-field case the EIT spectrum can be described for all values of parameters by a single formula* (5.7), where the substitution

$$\Gamma' \to \Gamma' + \nu \qquad (6.7)$$

is performed. This is illustrated by Figure 3a, where the plots calculated by the continued fraction (3.6) and by the result (5.7, 6.7) coincide.

In the strong-field case, *i.e.*, above the horizontal axis in Figure 1a, the transformation of the central part of the spectrum with ν is shown in Figure 2b (curve 1 in Fig. 2b is the central part of curve 3 in Fig. 2a). The central peak decreases with ν according to (6.6) in the interval $\Gamma^2\Gamma'/V_0^2 \ll \nu \ll \Gamma'^3/V_0^2$ (region II), as illustrated by Figure 2b, curve 2, and Figure 3b, the dotted line. The

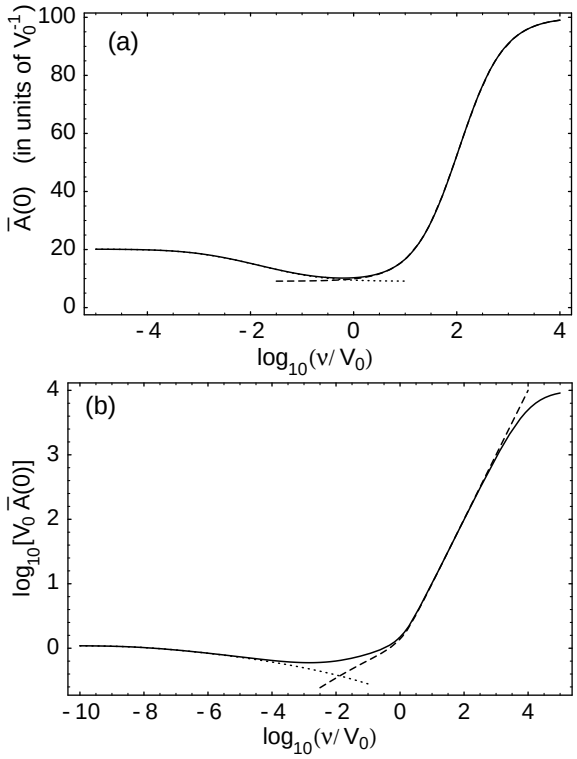

Fig. 3. Scaled resonant absorption $V_0\bar{A}(0)$ as a function of scaled bandwidth in a linear-log (a) and log-log (b) scales for the constructive-interference case: $\Gamma = 10^{-3}\Gamma'$, $\Delta_c = 0$. (a) Weak-field case, $\Gamma' = 10V_0$. Solid line, the calculation by the continued fraction (3.6) and the result (5.7, 6.7); dotted line, equation (5.7); dashed line, the result (4.12). (b) Strong-field case, $\Gamma' = 0.1V_0$. Solid line, numerical solution by (3.6); dotted line, equation (5.7); dashed line, solution with $\Gamma = \Gamma' = 0$ [10].

peak disappears at $\nu \sim \Gamma'^3/V_0^2$ (boundary 3 in Fig. 1a), so that only the Autler-Towns doublet remains. In regions III and IV (Fig. 1a) the lineshape is close to that obtained in the case (3.5) [10], as mentioned in Section (6.1). The dependence of the peak hight on ν for a strong coupling field is shown in Figure 3b.

As follows from the above discussion, in the strong-field case the transparency is maximal for $\nu \sim \nu_0 = \Gamma'^3/V_0^2$. Inserting the above estimation into equation (6.6), one obtains that the minimal absorption coefficient

$$\bar{A}_{\min} = \bar{A}(0)\big|_{\nu\sim\nu_0} \approx \frac{\Gamma'}{V_0^2}\ln\frac{V_0^2}{\Gamma'^2}\,. \qquad (6.8)$$

This value is larger by the factor $\ln(V_0^2/\Gamma'^2)$ than the absorption coefficient for a monochromatic coupling field of the same average intensity as the chaotic field. In contrast, recall that in the weak-field case the maximal transparency (achieved in region V) equals that induced by a monochromatic coupling field of the same average intensity.

6.2.2 TLS evolution

As follows from equation (2.8), the average evolution function $\bar{U}_{aa}(t)$ can be obtained by the inverse Laplace transform of $\hat{\bar{U}}_{aa}(s) = \bar{\Psi}_a\big|_{\Delta=is}$. Inserting equation (5.5) into the latter equality yields

$$\hat{\bar{U}}_{aa}(s) = \int_0^\infty q_0(s,t)\mathrm{e}^{-st}\mathrm{d}t, \qquad (6.9)$$

where $q_0(s,t) = \bar{g}(t)|_{\Delta=is}\,\mathrm{e}^{-\Gamma t}$.

In the weak field case (the region below the horizontal axis in Fig. 1a), as shown below, one can set $\Gamma' + s \approx \Gamma'$ in $\hat{\bar{U}}_{aa}(s)$, equation (6.9). Then $\hat{\bar{U}}_{aa}(s)$ becomes a Laplace transform of $q_0(0,t) = \bar{U}_{aa}(t)$, yielding

$$\bar{U}_{aa}(t) = \frac{4\beta_0'\mathrm{e}^{(\nu-\Gamma)t}}{2\beta_0'\cosh\beta_0'\nu t + (1+\beta_0'^2)\sinh\beta_0'\nu t}, \qquad (6.10)$$

where $\beta_0' = (1 + 2V_0^2/\nu\Gamma_c)^{1/2}$. The short- and long-time asymptotics of equation (6.10) are

$$\bar{U}_{aa}(t) \approx \bar{U}_{aa}^{\mathrm{st}}(t) \approx \frac{\mathrm{e}^{-\Gamma t}}{1 + V_0^2 t/\Gamma_c}, \quad |\beta_0'|\nu t \ll 1, \qquad (6.11a)$$

$$\bar{U}_{aa}(t) \approx \frac{4\beta_0'\mathrm{e}^{-[(\beta_0'-1)\nu+\Gamma]t}}{(1+\beta_0')^2}, \qquad \mathrm{e}^{|\beta_0'|\nu t} \gg 1. \qquad (6.11b)$$

The present approximation holds for $\Gamma' t \gg 1$. It is valid practically for all times, provided $\bar{U}_{aa}(1/\Gamma') \approx 1$, which is true for a weak field, $V_0 \ll \Gamma'$ (see Eq. (6.11a)). Note that equation (6.10) is similar to equation (34) in [7].

In the weak-field case, the static-limit evolution function (4.4) approximately equals equation (6.11a). When the bandwidth ν is so small that $|\beta_0|\nu \ll \Gamma$, which occurs in region I in Figure 1a, the static result (6.11a) describes actually the whole evolution. Outside region I one can neglect Γ in equations (6.10) and (6.11). In region II the static evolution function (6.11a) has a ν-dependent exponential cutoff at long times, as shown by equation (6.11b). In regions IV and V the broadband-limit result (4.16) is a good approximation to equation (6.10). The discussion in Section 6.2.1 implies that equation (6.10) with the substitution (6.7) determines the evolution function in the whole domain of the weak field.

Consider the strong-field case, $V_0 \gg \Gamma'$ (the upper half plane in Fig. 1a). In the static limit, as follows from the analysis of equation (4.4), the evolution function for $\Gamma' t \ll 1$ is given by equation (4.5), whereas

$$\bar{U}_{aa}^{\mathrm{st}}(t) \approx \left(\frac{\Gamma_c - \Gamma}{V_0^2 t} - \frac{1}{V_0^2 t^2}\right)\mathrm{e}^{-\Gamma t} \quad (2\Gamma' t \gg 1). \qquad (6.12)$$

For $\Delta_c = 0$, the function $\bar{U}_{aa}^{\mathrm{st}}(t)$ changes the sign twice (see Fig. 4, curve 1).

According to equations (6.11a, 6.12), $\bar{U}_{aa}^{\mathrm{st}}(t) \approx \Gamma_c\mathrm{e}^{-\Gamma t}/V_0^2 t$ for long times. This behaviour can be traced to the fact that the decay of $U_{aa}(t)$, equation (4.3), slows down with the decrease of V, so that $U_{aa}(t) \approx$

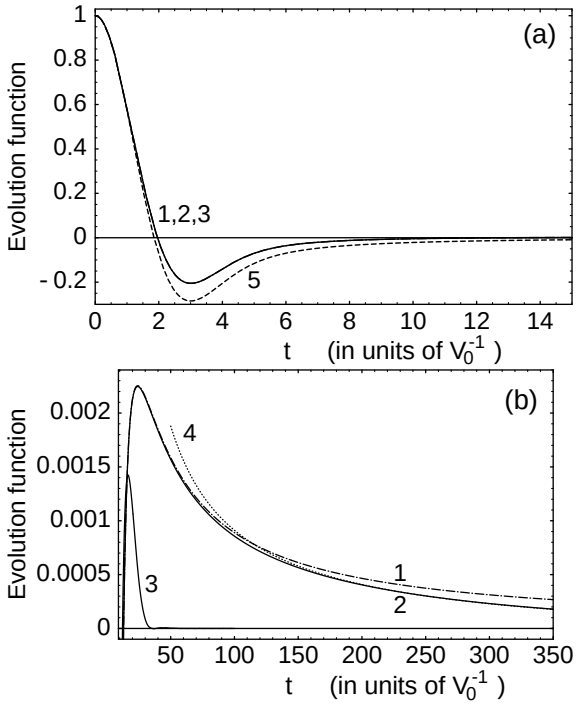

Fig. 4. The evolution function $\bar{U}_{aa}(t)$ for the constructive interference, strong-field case, $\Gamma = 10^{-4}V_0$, $\Gamma' = 0.1V_0$. Here $\Delta_c = 0$; $\nu/V_0 = 0$ (curve 1), 10^{-6} (curves 2 and 4), 0.0015 (curve 3). Curve 4, equations (6.13, 6.15); curve 5, equation (4.5) (*i.e.*, $\Gamma = \Gamma' = \nu = 0$). (a) Short times. (b) Long times.

$e^{-(\Gamma+V^2/\Gamma_c)t}$ for $V \ll \Gamma'$ and $t \gg 1/\Gamma'$. As a result, for $t \gg \Gamma'/V_0^2, 1/\Gamma'$, one can use the latter expression for $U_{aa}(t)$ and set $f(\mathbf{V}) \approx f(0)$ in $\bar{U}_{aa}^{st}(t) = \int U_{aa}(t)f(\mathbf{V})d\mathbf{V}$, which yields the above long-time result for $\bar{U}_{aa}^{st}(t)$.

Consider the effects of temporal coupling-field fluctuations on the evolution in the strong-field case. Regions III and IV, corresponding to the regime (3.5), were studied in [10]. Here we consider the time dependence in regions I and II. As in the weak-field case, in regions I and II the most part of the evolution occurs according to the static law, whereas the effect of the temporal fluctuations is to accelerate the decay at long times. The behavior at $t \gg \Gamma'^{-1}$ can be described roughly by equation (6.10). A better approximation (Appendix B) yields

$$\bar{U}_{aa}(t) \approx q_0(\sigma_0, t) \qquad (t \gg \Gamma'^{-1}), \tag{6.13}$$

where σ_0 satisfies the equation

$$\sigma_0 = -[\beta_0(\sigma_0) - 1]\nu - \Gamma \equiv h(\sigma_0). \tag{6.14}$$

An approximate solution of equation (6.14) is (Appendix B)

$$\sigma_0 \approx -(\beta_0' - 1)\nu - \Gamma. \tag{6.15}$$

The evolution functions corresponding to the lineshapes 1–3 in Figure 2b are shown in Figure 4, curves 1–3, respectively. As follows from Figure 4, the evolution function $\bar{U}_{aa}(t)$ in region II (curve 2) is very close to the static law (4.4) (curve 1), except for long times, where the effect of temporal fluctuations becomes significant. The latter limit is described fairly well by the result (6.13, 6.15) (curve 4). Curve 3 in Figure 4 shows the TLS evolution at the transition between regions II and III, $V_0^2\nu \sim \Gamma'^3$. The comparison of curves 2 and 3 shows that the decay accelerates with the increase of ν, which is expected in regions II and III. Figure 4 also shows, for comparison, the function (4.5) (curve 5).

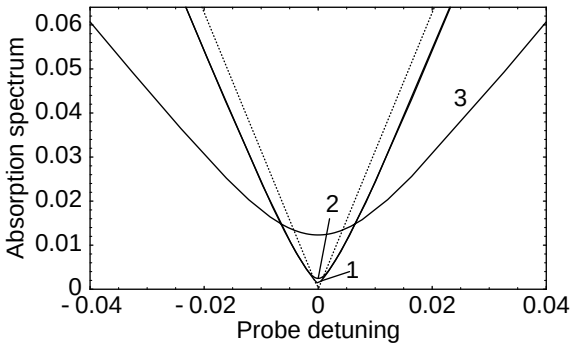

Fig. 5. The probe absorption spectrum $\bar{A}(\Delta)$ (in units of V_0^{-1}) as a function of the probe detuning Δ (in units of V_0) for the destructive interference, strong-field case, $\Gamma = 10^{-2}V_0$, $\Gamma' = 10^{-4}V_0$. Here $\Delta_c = 0$; $\nu/V_0 = 0$ (curve 1), 10^{-8} (curve 2), 10^{-6} (curve 3). Dotted curve, $\Gamma = \Gamma' = \nu = 0$ (Eq. (4.2)).

6.3 Destructive interference ($\Gamma \gg \Gamma'$)

6.3.1 EIT spectrum

In the destructive-interference case the EIT lineshape was found in [8] to be

$$\bar{A}(\Delta) = \frac{\Gamma}{\Gamma^2 + \Delta^2} - V_0^2 \mathrm{Re}\frac{F(2,1;1+d;-z)}{\tilde{\Gamma}^2[\tilde{\Gamma}' + (2\beta-1)\nu]}, \tag{6.16}$$

where $z = (\beta-1)^2/(4\beta)$, $d = [(2\beta-1)\nu + \tilde{\Gamma}']/(2\beta\nu)$, and $\beta = \sqrt{1 + 2V_0^2/(\nu\tilde{\Gamma})}$. Equation (6.16) holds under condition (6.3) with $\Gamma_+ = \Gamma$ [8], *i.e.*, in the sector between line 3 and the negative vertical half axis (Fig. 1b), which comprises regions I and II.

The lineshape (6.16) was studied in detail in [8]. Expression (6.16) describes completely the weak-field case, $V_0 \ll \Gamma$, and partially the strong-field case, $V_0 \gg \Gamma$. In regions I and II, the spectrum has a minimum at $\Delta \approx -\Delta_c$, which is significantly affected by destructive interference. For $\sqrt{V_0^2\nu} \ll \Gamma'\sqrt{\Gamma}$ (region I in Fig. 1b) the lineshape is approximately static, whereas in region II the absorption coefficient at the minimum is proportional to $\sqrt{\nu}$. Figure 5 shows the strong-field EIT lineshapes (near the minimum) in regions I, II, and at the transition between regions II and III (curves 1–3, respectively). For comparison, the spectrum (4.2) is also shown (the dotted curve).

The absorption coefficient at the probe resonance for a strong coupling field is plotted *versus* ν in Figure 6 (the

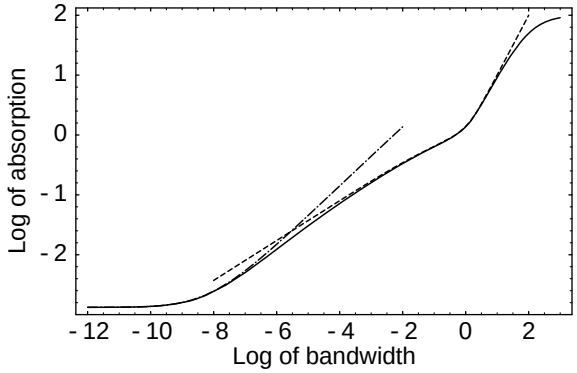

Fig. 6. Scaled resonant absorption *versus* scaled bandwidth in a logarithmic scale: $\log_{10}[V_0\bar{A}(0)]$ *versus* $\log_{10}(\nu/V_0)$, for the destructive interference, strong-field case, $\Gamma = 10^{-2}V_0$, $\Gamma' = 10^{-4}V_0$, $\Delta_c = 0$. Solid line, numerical solution by (3.6); dot-dashed line, equation (6.16); dashed line, case $\Gamma = \Gamma' = 0$ [10].

solid line). For comparison, Figure 6 shows also the plots of equation (6.16) (the dot-dashed line) and the result corresponding to the case (3.5) [10] (the dashed line). In particular, Figure 6 demonstrates the crossover at $\nu \sim \Gamma^3/V_0^2$ between the $\nu^{1/2}$ and $\nu^{1/3}$ scalings pertinent, respectively, to regions II and III in Figure 1b. The transition between regions III and IV (which occurs at $V_0 \sim \nu$) is rather sharp, whereas for larger ν (region IV and beyond it) the broadband-limit result (4.10) holds, as discussed above.

6.3.2 TLS evolution

We turn now to the time domain. Using equation (6.11) of [8] (with a misprint corrected: the factor $\tilde{\Gamma}^{-1}$ should be inserted before the integral), one obtains, similarly to equation (6.9),

$$\hat{\bar{U}}_{aa}(s) = \frac{1}{\Gamma + s} - \int_0^\infty q(s,t)\mathrm{e}^{-st}\mathrm{d}t. \qquad (6.17)$$

Here $q(s,t) = 4V_0^2\beta^2(s)\mathrm{e}^{(\nu-\Gamma_c)t}/[(\Gamma+s)S(\beta(s),t)]^2$, where $\beta(s) = [1 + 2V_0^2/\nu(\Gamma + s)]^{1/2}$.

In the weak-field case, the evolution function can be found as follows. For short times, $t \ll \Gamma/V_0^2, 1/\nu$, one obtains that $\mathrm{e}^{(\nu-\Gamma_c)t} \approx 1$ and $S(\beta(s),t) \approx 2\beta(s)$. This yields $q(s,t) \approx V_0^2/(\Gamma + s)^2$ and hence the second term on the right-hand side (rhs) of equation (6.17) is approximately $-V_0^2/s(\Gamma + s)^2$. The inverse Laplace transform of equation (6.17) in this case can be performed readily. On the other hand, for $t \gg 1/\Gamma$ the inverse Laplace transform of the first term on the rhs of equation (6.17), $\mathrm{e}^{-\Gamma t}$, practically vanishes, whereas in the second term one can set $s \approx 0$, yielding $\bar{U}_{aa}(t) \approx -q(0,t)$. The interpolation formula which incorporates the both limits is

$$\bar{U}_{aa}(t) = (1 + V_0^2/\Gamma^2 + V_0^2 t/\Gamma)\mathrm{e}^{-\Gamma t} - q(0,t). \qquad (6.18)$$

For a weak field, $V_0^2 \ll \Gamma^2$, with $\nu \ll \Gamma$, the above limits overlap, which means that equation (6.18) holds for all times.

According to equation (6.18), the evolution function first decreases fast (with the rate Γ) from 1 to $-V_0^2/\Gamma^2$ and then slowly decays to zero. Equation (6.18) has the following short- and long-time behavior,

$$\bar{U}_{aa}(t) \approx \bar{U}^{\mathrm{st}}_{aa}(t) \approx (1 + V_0^2/\Gamma^2 + V_0^2 t/\Gamma)\mathrm{e}^{-\Gamma t} - V_0^2\mathrm{e}^{-\Gamma_c t}/(\Gamma + V_0^2 t)^2, \quad \beta'\nu t \ll 1, \qquad (6.19a)$$

$$\bar{U}_{aa}(t) \approx -\frac{16V_0^2\beta'^2\mathrm{e}^{-(2\beta'-1)\nu t-\Gamma_c t}}{\Gamma^2(1+\beta')^4}, \quad \mathrm{e}^{\beta'\nu t} \gg 1, \qquad (6.19b)$$

where $\beta' = (1 + 2V_0^2/\nu\Gamma)^{1/2}$. Equation (6.19a) describes the static decay in the weak-field case. According to equation (6.19a), for $t \gg \Gamma/V_0^2$

$$\bar{U}^{\mathrm{st}}_{aa}(t) \approx -\mathrm{e}^{-\Gamma_c t}/(V_0 t)^2, \qquad (6.20)$$

i.e., for long times the evolution function decays as $-t^{-2}$ until the exponential cutoff at $t \sim \Gamma'^{-1}$. The static result (6.19a) is responsible practically for the whole evolution in region I ($\Gamma' \gg \beta'\nu$). In region II the static $-t^{-2}$ decay has a ν-dependent exponential cutoff described by equation (6.19b).

Consider now the strong-field case. In the static limit, equation (4.4) implies that $\bar{U}^{\mathrm{st}}_{aa}(t)$ is given by equation (4.5) for $t \ll \Gamma^{-1}$ and by equation (6.20) for $t \gg \Gamma^{-1}$. As in the weak-field case, in region II the TLS evolution is sensitive to ν only at long times. The approximate formula for the long-time behavior in regions I and II can be obtained, as follows. For $t \gg \Gamma^{-1}$ the inverse transform of the first term on the rhs of equation (6.17), $\mathrm{e}^{-\Gamma t}$, is negligible. The inverse transform of the second term for $t \gg \Gamma^{-1}$ is performed analogously to the derivation of equation (6.13), yielding

$$\bar{U}_{aa}(t) \approx -q(\sigma,t) \qquad (t \gg \Gamma^{-1}), \qquad (6.21a)$$

where σ satisfies the equation $\sigma = -[2\beta(\sigma) - 1]\nu - \Gamma_c$. In the first approximation one obtains

$$\sigma \approx -(2\beta' - 1)\nu - \Gamma_c. \qquad (6.21b)$$

The plots of $\bar{U}_{aa}(t)$ in regions I and II (Fig. 1b) for the strong-field case are shown in Figure 7, curves 1 and 2, respectively. These plots are obtained by the Fourier transform (6.4) of the spectra shown in Figure 5 (curves 1 and 2). The main part of the static evolution (curve 1) coincides with the relaxationless static result (4.5) (the dashed line), whereas for long times curve 1 coincides with the dotted line (Eq. (6.20)). The evolution function in region II (curve 2) is close to the static result (curve 1), except for very long times where temporal fluctuations result in an acceleration of the decay. The latter stage is described fairly well by equation (6.21) (the dot-dashed line in Fig. 7).

6.4 Comparable relaxation constants

In the case $\Gamma \sim \Gamma'$, the boundaries of different regimes can be obtained from Figure 1b by moving boundaries 1

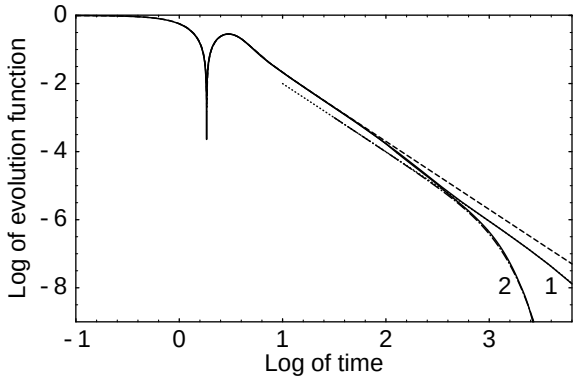

Fig. 7. The evolution function in a logarithmic scale: $\log_{10}|\bar{U}_{aa}(t)|$ *versus* $\log_{10}(V_0 t)$, for the destructive interference, strong-field case, $\Gamma = 10^{-2}V_0$, $\Gamma' = 10^{-4}V_0$, $\Delta_c = 0$. Here $\nu/V_0 = 0$ (solid curve 1), 10^{-8} (solid curve 2). Dashed line, equation (4.5); dotted line, equation (6.20); dot-dashed line, equation (6.21).

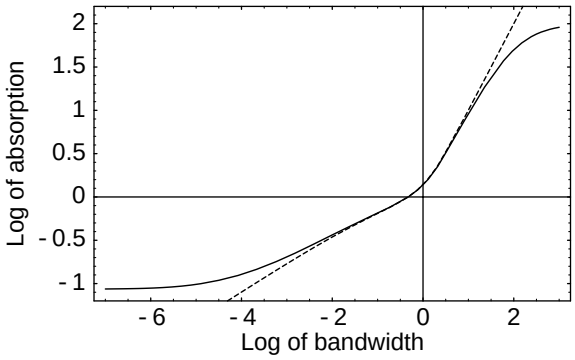

Fig. 8. Scaled resonant absorption *versus* scaled bandwidth in a logarithmic scale: $\log_{10}[V_0\bar{A}(0)]$ *versus* $\log_{10}(\nu/V_0)$, for $\Delta_c = 0$. Solid line, $\Gamma = \Gamma' = 0.01V_0$; dashed line, $\Gamma = \Gamma' = 0$ [10].

and 2 up to their merging with the negative abscissa axis and boundary 3, respectively. This implies that region II disappears, whereas boundary 3 ($V_0^2\nu = \Gamma^3$) separates regions I and III. Now a significant EIT can be produced only by a strong coupling field, $V_0 \gg \Gamma$. Henceforth, we focus, for simplicity, on the case $\Gamma = \Gamma'$, $\Delta_c = 0$.

In the static limit, as follows from equation (4.4), the evolution function is given by the product of equation (4.5) and the factor $e^{-\Gamma t}$, which provides a cutoff at long t.

Correspondingly, in the static limit the spectrum is close to equation (4.2), except for a narrow vicinity of $\Delta = 0$ where the lineshape is smoothed. More specifically, as follows from equation (4.1), for $|\Delta| \ll V_0$ the lineshape is [8,9]

$$\bar{A}(\Delta) = \frac{1}{V_0^2}\left(\Gamma \ln\frac{C_1 V_0^2}{\Gamma^2+\Delta^2} + 2\Delta \arctan\frac{\Delta}{\Gamma}\right). \quad (6.22)$$

The absorption is minimal at $\Delta = 0$, where $A(0) = (\Gamma/V_0^2)\ln(C_1 V_0^2/\Gamma^2)$, which is greater by the logarithmic factor than the absorption coefficient with a monochromatic coupling field of the same average intensity.

The maximum EIT, given by $\bar{A}(0)$, is plotted *versus* ν in Figure 8. In accordance with the above discussion, the increase of ν leads to the transition from the ν-independent static limit to the relaxationless regime (the dashed line) and then to the unperturbed case (a negligible coupling field).

7 Conclusion

Above we have studied the EIT and the average (reduced) evolution of a TLS under a (near-)resonant chaotic field. The general solution in the form of a continued fraction has been obtained and used for numerical calculations. Moreover, a number of analytical results for special cases have been derived. The present results, together with the previous ones [8–10], describe analytically all the regimes. Only the transition region $V_0^2\nu \sim (\Gamma+\Gamma')^3$ in the strong-field case, $V_0 \gtrsim \Gamma+\Gamma'$, cannot be described analytically. The results have been verified by numerical calculations. As a result, a comprehensive picture of the EIT and the TLS evolution have been obtained.

The results of the broadband limit (the part of the parameter space to the right of boundaries 4 and 5 in Figure 1, including regions IV and V) have been shown to hold for a rather general class of stochastic fields. The quasistatic results (region I) are also rather general, as mentioned above. In contrast, the behavior in regions II and III (as well as the boundary between regions I and II) significantly depends on the specific model of the stochastic field [8,10].

In the constructive-interference case, the counterintuitive fact has been obtained that the EIT increases with the field bandwidth for sufficiently small bandwidths[2] (Sect. 6.2). As a result, in the strong-field case the EIT is maximal for a certain optimal bandwidth. The minimal absorption coefficient is greater than that for a monochromatic field of the same average intensity, the discrepancy increasing with the field.

In contrast, in the weak-field case there is a *range* of values of ν, where the EIT is maximal. Moreover, in this region the effect of the field fluctuations on the spectrum and the evolution function is *negligible*. This regime pertains to the broadband limit and therefore should hold for stochastic fields more general than the chaotic field, as discussed above.

The present research was supported by the Ministry of Absorption *via* the Center for Absorption of Scientists.

Appendix A: Validity conditions of equation (5.7)

The expressions (5.3) and (5.1) are the zero-order solutions, $\Psi_a^{(0)}$ and $\Psi_b^{(0)}$, respectively, of equations (2.6). To

[2] For the strong-field case, this fact was first revealed in [9].

find corrections to these solutions, we cast equation (2.6b) in the integral form,

$$-\tilde{\Gamma}'\Psi_b - \mathrm{i}V_\mathrm{c}\Psi_a = \mathrm{i}\tilde{\Gamma}' \int \mathrm{d}\mathbf{V}' V_\mathrm{c}'\Psi_a(\mathbf{V}')F(\mathbf{V}',\mathbf{V}) - \mathrm{i}V_\mathrm{c}\Psi_a, \tag{A.1}$$

where $F(\mathbf{V}',\mathbf{V}) = \int_0^\infty \mathrm{d}t f(\mathbf{V}';\mathbf{V},t)\mathrm{e}^{-\tilde{\Gamma}'t}$. Here $f(\mathbf{V}';\mathbf{V},t)$ is the conditional probability of the random process $\mathbf{V}(t)$ (see Ref. [8], Eqs. (B4, B5)).

The zero-order solution is obtained when the rhs of equation (A.1) vanishes. The functions $\Psi_{a(b)}^{(1)}(\mathbf{V})$, involving the first-order corrections, appear on the left-hand sides of the set of equations (2.6a, A.1), on inserting $\Psi_a \approx \Psi_a^{(0)}$ on the rhs of equation (A.1). Then solving equation (A.1) for $\Psi_b^{(1)}(\mathbf{V})$ and inserting the result into equation (2.6a) yields

$$-\tilde{\Gamma}\Psi_a^{(1)} - \frac{V^2}{\tilde{\Gamma}'}\Psi_a^{(1)} + L\Psi_a^{(1)} = -f(V) + V_\mathrm{c}^* \int \mathrm{d}\mathbf{V}' V_\mathrm{c}'\Psi_a^{(0)}(\mathbf{V}')F(\mathbf{V}',\mathbf{V}) - \frac{V^2}{\tilde{\Gamma}'}\Psi_a^{(0)}. \tag{A.2}$$

Let us now estimate $\Psi_a^{(0)}(\mathbf{V})$, equation (5.3). Equation (5.6) implies that

$$g(\mathbf{V},t) \approx f(V)\mathrm{e}^{-V^2 t/\tilde{\Gamma}'}, \quad |\beta_0|\nu t \ll 1, \tag{A.3a}$$

$$g(\mathbf{V},t) \approx f(V)\exp[-\beta_0\nu t - (\beta_0 - 1)V^2/2V_0^2], \quad \mathrm{e}^{|\beta_0|\nu t} \gg 1. \tag{A.3b}$$

Using equations (A.3) in equation (5.3), one can obtain that $\Psi_a^{(0)}(\mathbf{V}) \sim f(V)/(\tilde{\Gamma} + \beta_0\nu)$ for $V^2 \lesssim |\beta_0\nu\tilde{\Gamma}'|$ and $\Psi_a^{(0)}(\mathbf{V}) \approx f(V)\tilde{\Gamma}'/(V^2 + \tilde{\Gamma}\tilde{\Gamma}')$ for $V^2 \gg |\beta_0\nu\tilde{\Gamma}'|$. This can be recast as follows,

$$|\Psi_a^{(0)}(\mathbf{V})| \sim f(V)|\tilde{\Gamma}'|/V_1^2, \quad V \ll V_1$$
$$\Psi_a^{(0)}(\mathbf{V}) \approx f(V)\tilde{\Gamma}'/V^2, \quad V \gg V_1, \tag{A.4}$$

where V_1 is the width of $\Psi_a^{(0)}(\mathbf{V})/f(V)$ as a function of V, $V_1^2 = |\beta_0\nu\tilde{\Gamma}'| + |\tilde{\Gamma}\tilde{\Gamma}'|$.

As follows from the form of $f(\mathbf{V}';\mathbf{V},t)$ [8], in the case (5.8b) $F(\mathbf{V}',\mathbf{V})$ as a function of $\mathbf{V}'$ is a bell-like function centered at $\mathbf{V}$ with the width $V_F = \sqrt{V_0^2\nu/|\tilde{\Gamma}'|}$. When $V_F \ll V_1$, one can approximate $F(\mathbf{V}',\mathbf{V}) \approx \delta(\mathbf{V} - \mathbf{V}')/\tilde{\Gamma}'$ in the second term on the rhs of equation (A.2). This implies that the modulus of the sum of the last two terms on the rhs of equation (A.2) is much less than $V^2|\Psi_a^{(0)}(\mathbf{V})/\tilde{\Gamma}'| \sim f(V)$ (the latter relation follows from (A.4)). The above inequality means that equation (A.2) approximately coincides with (5.2), which yields in turn that $\Psi_a^{(1)}(\mathbf{V}) \approx \Psi_a^{(0)}(\mathbf{V})$. Note that the condition $V_F \ll V_1$ is equivalent to equation (5.8a). Thus we have proved the validity of equation (5.7) under the conditions (5.8).

Appendix B: Approximate inverse transform of equation (6.9)

The inverse Laplace transform of the evolution function is given by

$$\bar{U}_{aa}(t) = \frac{1}{2\pi}\int_{-\infty}^{\infty} \hat{\bar{U}}_{aa}(\sigma + \mathrm{i}\lambda)\mathrm{e}^{(\sigma+\mathrm{i}\lambda)t}\mathrm{d}\lambda, \tag{B.1}$$

where σ is such that the integration contour in equation (B.1) is to the right of all the singularities of $\hat{\bar{U}}_{aa}(s)$. We look for the minimal σ, *i.e.*, such σ that the integration contour is as close as possible to the rightist pole of $\hat{\bar{U}}_{aa}(s)$. Taking into account that $q_0(s,t) \sim \mathrm{e}^{-[\beta_0(s)-1]\nu t - \Gamma t}$ for $t \to \infty$, where $\beta_0(s) = [1+2V_0^2/\nu(\Gamma_\mathrm{c}+s)]^{1/2}$, one observes that the minimal $s = \sigma_0$, for which the integral in (6.9) converges, satisfies the equation (6.14). For $t \gg \Gamma'^{-1}$ and $\sigma = \sigma_0$, the main contribution to the integral in equation (B.1) is obtained from λ such that $|\lambda| \ll \Gamma' \approx \Gamma' + \sigma_0$. For such λ, in equation (6.9) $q_0(s = \sigma_0 + \mathrm{i}\lambda, t) \approx q_0(\sigma_0, t)$, and hence (6.9) has the form of the Laplace transform of $q_0(\sigma_0, t)$. This means that the inverse transform will yield equation (6.13).

On expanding $h(\sigma_0)$, equation (6.14), in powers of σ_0, one obtains that in the second approximation $\sigma_0 = h(0)[1 + h'(0)]$, where $h'(\sigma) = \mathrm{d}h/\mathrm{d}\sigma$. One can show that $h'(0) \sim (V_0^2\nu/\Gamma'^3)^{1/2} \ll 1$. Therefore $\sigma_0 \approx h(0)$, yielding equation (6.15).

References

1. K.-J. Boller, A. Imamoğlu, S.E. Harris, Phys. Rev. Lett. **66**, 2593 (1991); J.E. Field, K.H. Hahn, S.E. Harris, Phys. Rev. Lett. **67**, 3062 (1991); Y. Li, M. Xiao, Phys. Rev. A **51**, 4959 (1995); S.E. Harris, Phys. Today **50**, 36 (1997); F.S. Cataliotti, C. Fort, T.W. Hänsch, M. Inguscio, M. Prevedelli, Phys. Rev. A **56**, 2221 (1997); L.V. Hau, S.E. Harris, Z. Dutton, C.H. Behroosi, Nature **397**, 594 (1999); D. Budker, D.F. Kimball, S.M. Rochester, V.V. Yashchuk, Phys. Rev. Lett. **83**, 1767 (1999).
2. S.P. Tewari, G.S. Agarwal, Phys. Rev. Lett. **56**, 1811 (1986); S.E. Harris, J.E. Field, A. Imamoğlu, *ibid.* **64**, 1107 (1990); G.Z. Zhang, K. Hakuta, B.P. Stoicheff, *ibid.* **71**, 3099 (1993); L. Deng, M.G. Payne, W.R. Garrett, Opt. Commun. **126**, 73 (1996); W. Harshawardhan, G.S. Agarwal, Phys. Rev. A **53**, 1812 (1996); A. Kasapi, Phys. Rev. Lett. **77**, 1035 (1996).
3. L.D. Zusman, A.I. Burshtein, Zh. Eksp. Teor. Fiz. **61**, 976 (1971) [Sov. Phys. JETP **34**, 520 (1972)].
4. J. Gea-Banacloche, Y. Li, S. Jin, M. Xiao, Phys. Rev. A **51**, 576 (1995); B. Lü, W.H. Burkett, M. Xiao, Phys. Rev. A **56**, 976 (1997).
5. S.G. Przhibelskii, Opt. Spektrosk. **35**, 715 (1973) [Opt. Spectrosc. **35**, 415 (1973)].
6. P.V. Elyutin, Opt. Spektrosk. **43**, 542 (1977) [Opt. Spectrosc. **43**, 318 (1977)]; Sov. Phys. Dokl. **22**, 390 (1977) [Dokl. Akad. Nauk SSSR **235**, 317 (1977)].
7. N.F. Perelman, I.Sh. Averbukh, V.A. Kovarsky, Zh. Eksp. Teor. Fiz. **93**, 483 (1987) [Sov. Phys. JETP **66**, 276 (1987)].

8. A.G. Kofman, Phys. Rev. A **56**, 2280 (1997).
9. A.G. Kofman, Europhys. Lett. **46**, 164 (1999).
10. A.G. Kofman, Phys. Rev. A **63**, 033810 (2001).
11. G.S. Agarwal, G. Vemuri, Phys. Rev. A **55**, 1466 (1997)
12. F. Bernardot, P. Nussenzveig, M. Brune, J.M. Raimond, S. Haroche, Europhys. Lett. **17**, 33 (1992); J.J. Childs, K. An, M.S. Otteson, R.R. Dasari, M.S. Feld, Phys. Rev. Lett. **77**, 2901 (1996); R.J. Thompson, Q.A. Turchette, O. Carnal, H.J. Kimble, Phys. Rev. A **57**, 3084 (1998).
13. H. Carmichael, *An Open Systems Approach to Quantum Optics* (Springer, Berlin, 1993); G.C. Hegerfeldt, Phys. Rev. A **47**, 449 (1993); J. Dalibard, Y. Castin, K. Molmer, Phys. Lett. **68**, 580 (1992).
14. S. Mukamel, *Principles of Nonlinear Optical Spectroscopy* (Oxford, New York, 1995).
15. R. Zwanzig, Physica **30**, 1109 (1964); P.N. Argyres, P.L. Kelly, Phys. Rev. **134**, A98 (1964).
16. R.H. Terwiel, Physica **74**, 248 (1974); B. Yoon, J.M. Deutch, J.H. Freed, J. Chem. Phys. **62**, 4687 (1975); B.T.M. Roerdink, Physica A **109**, 23 (1981).
17. A.G. Kofman, R. Zaibel, A.M. Levine, Y. Prior, Phys, Rev. A **41**, 6434 (1990).
18. A.G. Kofman, Phys. Rev. A **63**, 033810 (2001).
19. F. Shibata, I. Sato, Physica A **143**, 468 (1987).
20. *Handbook of Mathematical Functions*, Natl. Bur. Stand. Appl. Math. Ser. No. 55, edited by M. Abramowitz, I.A. Stegun (U.S. GPO, Washington, DC, 1964).
21. A.I. Burshtein, A.G. Kofman, Zh. Eksp. Teor. Fiz. **70**, 840 (1976) [Sov. Phys. JETP **43**, 436 (1977)].
22. P. Zoller, P. Lambropoulos, J. Phys. B **13**, 69 (1980).